ACADEMIA ROMÂNĂ
Revue Roumaine de Chimie
http://web.icf.ro/rrch/

Rev. Roum. Chim.,
2017, *62*(12), 885-895

PAPERS

EFFECT OF VOLUME RATIO AND TEMPERATURE ON CORROSION BEHAVIOR OF DUPLEX STAINLESS STEEL AISI 2205 IN ETHYLENE GLYCOL-WATER MIXTURE

Ahmad GOODARZI, Iman DANAEE,* Hadi ESKANDARI and Soudabeh NIKMANESH

Abadan Faculty of Petroleum Engineering, Petroleum University of Technology, Abadan, Iran

Received April 17, 2016

The electrochemical behavior of Duplex stainless steel AISI 2205 in ethylene glycol-water mixture at different concentrations and different temperature was investigated by polarization, AC impedance measurements and scanning electron microscopy (SEM). The polarization curves showed Tafel type behavior of these samples in the active state. The results showed that with an increase in concentration of ethylene glycol to 10 V/V%, the corrosion rate of steel alloy substrate increased. In higher concentration of ethylene glycol, the corrosion rate of stainless steel substrate decreased. Electrochemical impedance spectroscopy (EIS) at different concentrations showed that the double layer capacitance tends to decrease as the ethylene glycol concentrations increased. The effect of temperature was studied and it was obtained that the corrosion rate increased with an increase in temperature. In addition, thermodynamic parameters were calculated in different ethylene glycol concentrations.

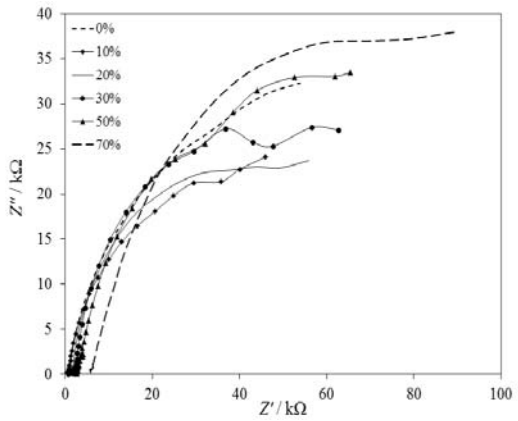

INTRODUCTION

Stainless steels often offer an economical combination of strength and corrosion resistance.[1,2] Duplex austenitic-ferric stainless steels are vastly used in petroleum industries, particularly for submarine gas and oil lines and other offshore applications because of their reasonable cost, good mechanical and thermal properties, and resistance to stress corrosion and pitting.[3] It is well known that such good properties depend on the two-phase microstructure consisting of approximately equal amounts of austenite (γ) and δ-ferrite.[3,4]

Water-based heat transfer fluids are formulated primarily with ethylene glycol and propylene glycol.[5] Ethylene glycol is the standard heat-transfer fluid for most industrial applications. The addition of ethylene glycol/water solutions increases the cooling capacity of the circulating fluid by allowing the cooling fluid to be cooled below 0°C.[6] Also ethylene glycol is widely used as coolant in automotive heat exchangers,

* Corresponding author: danaee@put.ac.ir ; Tel: 00986153329937

mixed with water, in a pH range between 7 and 8, due to its great heat absorption capacity.[7-9]

Corrosion investigations in ethylene glycol water mixtures have been performed on ferrous and non-ferrous alloy metals.[10-17] John *et al.*[16] investigated the corrosion behavior of magnesium in ethylene glycol. They concluded that the corrosion rate of magnesium decreased with increasing concentration of ethylene glycol. In addition, similar results were obtained by Fekry *et al.*[17] The cheapest and first structural material candidate one can have is carbon steel. Corrosion of steel and its alloys has been studied extensively in ethylene glycol water solution.[10-13] Guilminot *et al.*[14] investigated the iron corrosion in water–PEG 400 solutions by monitoring the corrosion potential and the polarization curves. Iron corrosion was highest in the 20% PEG 400 solution. Carbon steel is not precisely the most corrosion resistant for many environments. For this reason, the expected high corrosion rate of steel in aqueous solutions guides us to use stainless steel.[14,15]

The objective of the present work was to study the corrosion behavior of duplex stainless steel AISI 2205 in the ethylene glycol-water mixture at different concentrations of ethylene glycol and different temperatures by means of electrochemical measurements such as electrochemical impedance spectroscopy (EIS) and polarization tests. Also the surface morphology of the electrode surface was evaluated by scanning electron microscopy. Thermodynamic parameters for different concentration of ethylene glycol were calculated.

MATERIALS AND METHODS

Sodium chloride and ethylene glycol used in this work were prepared from Merck products of analytical grade and were used without further purifications. Doubly distilled water was used throughout. The experimental tested material was Duplex stainless steel AISI 2205 with nominal chemical composition in Table 1.

Samples for electrochemical experiments were cut in cubic dimensions by a wire cut machine. Each sample was sealed by polyester resin so leaving an approximate area of 1 cm^2 to be exposed to the electrolyte. The exposed areas of the electrodes were mechanically abraded with 220, 400, 600, 800, 1000 grades of emery paper, degreased with acetone and rinsed by distilled water before each electrochemical experiment. Corrosion tests were carried out in 100 ppm NaCl aqueous solution at different concentration of ethylene glycol to simulate the automotive heat exchangers and heat transfer fluids. The surface morphology of the electrode surface was evaluated by scanning electron microscopy model VEGA, TESCAN. Polarization and EIS tests were performed by Ivium poentiostat/galvanostat. In all electrochemical tests, before recording, the working electrode was maintained at its open circuit potential for 30 min until a steady state was obtained.

Electrochemical measurements were carried out in a conventional three electrode glass cell. Platinum electrode was used as a counter electrode and a saturated calomel electrode (SCE) as the reference electrode. Polarization curves were obtained by polarizing the specimens at a scanning rate of 1 m Vs^{-1}. Signals in EIS measurements were applied in the frequency range from 100 kHz to 10 mHz with peak-to-peak AC amplitude of 10 mV. All impedance data were measured at open circuit potential (OCP). Fitting of experimental impedance spectroscopy data to the proposed equivalent circuit was done by means of ZSim software.

RESULTS AND DISCUSSION

Polarization curves of steel electrode measured in solutions with different concentrations of ethylene glycol are shown in Fig. 1. The polarization curves show Tafel type behavior of these samples in the active state. Tafel calculations are listed in Table 2, where E_{corr}, I_{corr}, R_p, β_a, β_c and CR are the corrosion potential, corrosion current density, polarization resistance, anodic Tafel constant, cathodic Tafel constant and corrosion rate, respectively.

It can be seen from Fig. 1 and Table 2 that corrosion potentials shift to more positive values with increase in concentration of ethylene glycol. With increasing ethylene glycol concentration to 10%, corrosion current of steel alloy increases which is due to autoprotolysis of ethylene glycol caused by interactions between ethylene glycol and the water which leads to increasing production of ionic species.[14] In higher concentration of ethylene glycol, corrosion current of substrate decreases. More ethylene glycol molecules will be adsorbed on the surface in the higher concentrations of ethylene glycol, leading to decreasing the corrosion current density.[18]

Table 1

Chemical composition of material tested

Element	C max	Si max	Mn max	P max	S max	Cr	Ni	Mo	N
Wt.%	0.03	1.0	2.0	0.03	0.015	22	5	3.2	0.18

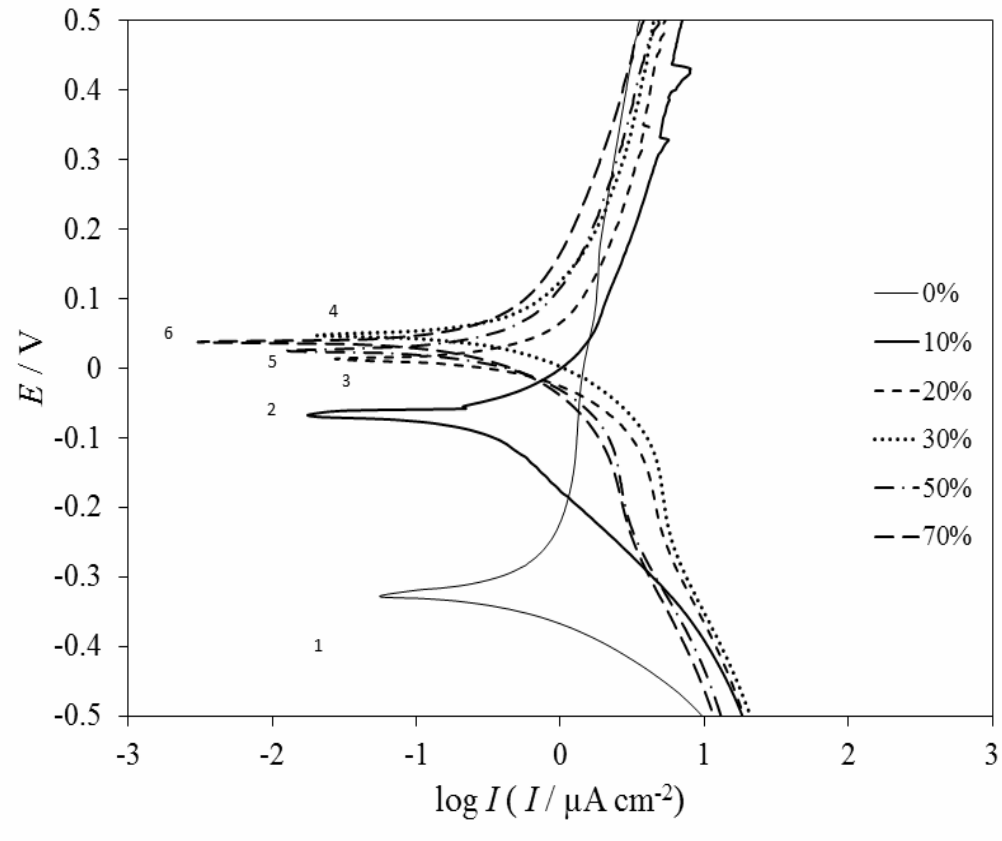

Fig. 1 – Polarization curves of duplex steel alloy electrode in 100 ppm NaCl and ethylene glycol-water solution with different concentrations of ethylene glycol: 1: 0 ; 2: 10; 3: 20; 4: 30; 5: 50; 6: 70 %V/V ethylene glycol.

Table 2

Polarization parameters in the corrosion of duplex stainless steel 2205 in 100 ppm NaCl and ethylene glycol-water solution at different concentrations of ethylene glycol

Ethylene glycol V/V %	0	10	20	30	50	70
E_{corr} / V	-0.326	-0.075	0.014	0.068	0.025	0.032
I_{corr} / μA cm^{-2}	0.197	0.551	0.233	0.191	0.139	0.112
R_p / kΩ	63.6	40.1	64.1	76.9	88.6	121.1
β_a / V dec^{-1}	0.073	0.185	0.11	0.11	0.067	0.083
β_c / V dec^{-1}	0.048	0.07	0.05	0.051	0.049	0.05
CR / mm year^{-1}	0.002292	0.006388	0.002702	0.002282	0.001615	0.001296

Fig. 2 shows the morphologies of the electrode surface in 10%, 30% and 70% ethylene glycol-water solution which obtained after holding the electrode at potential +1 V versus SCE for 1500 s. From Fig. 2 it can be concluded that with increasing in concentration of ethylene glycol, corrosion attack decreases. It is clear that, the surface is smoother in solutions containing 70% ethylene glycol.

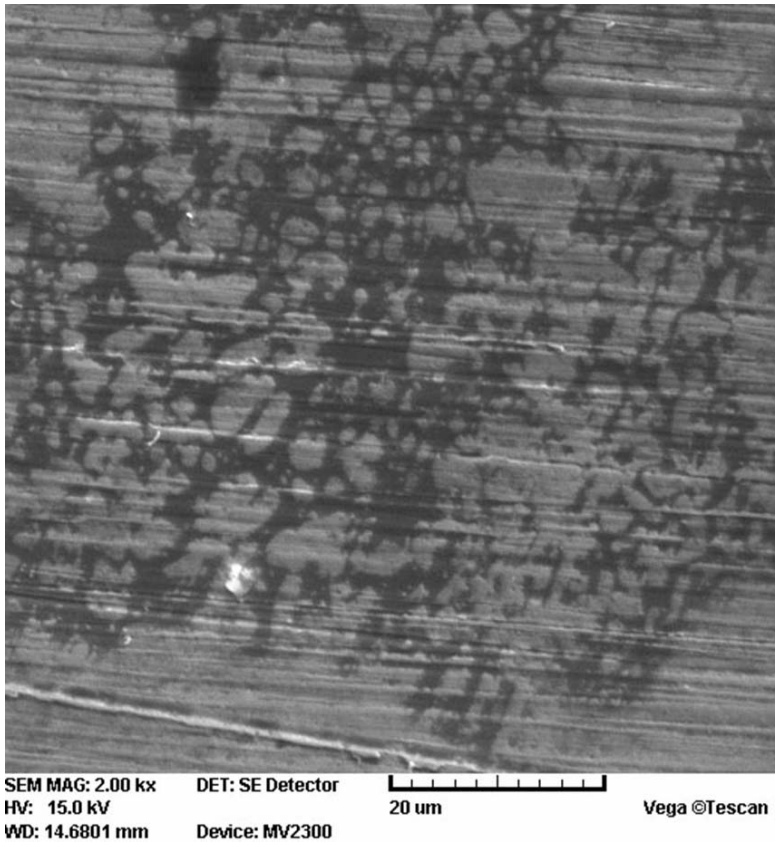

Figure 2a

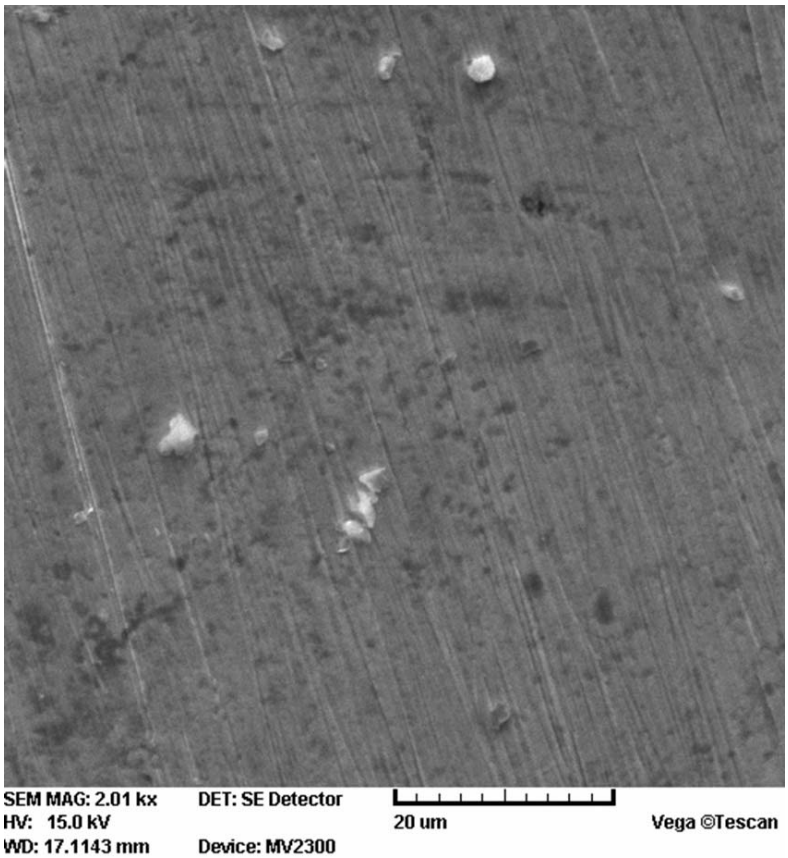

Figure 2b

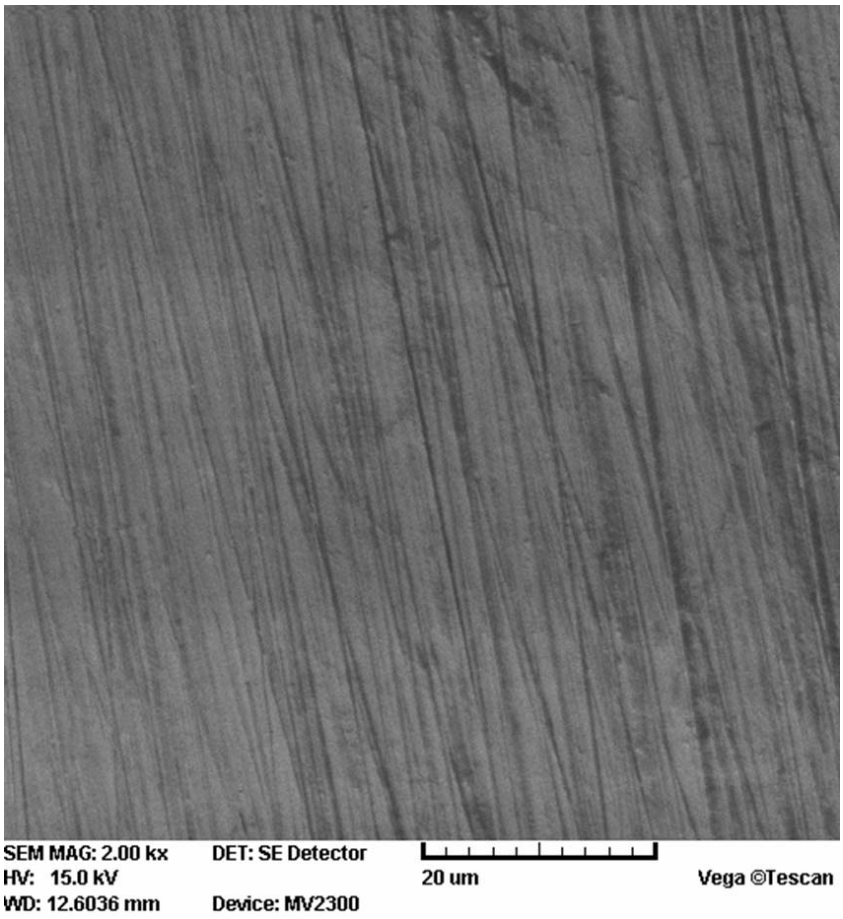

Figure 2c

Fig. 2 – Surface of duplex steel alloy electrode by metallographic microscope in 100 ppm NaCl and ethylene glycol-water solution at different concentrations of ethylene glycol: a: 10; b: 30; c:70 %V/V ethylene glycol.

In order to get more information about the corrosion phenomena, solution resistance (R_s), charge-transfer resistance (R_{ct}) and double layer capacitance (C_{dl}) of steel electrode, impedance measurements have been carried out in the presence of the different concentrations of ethylene glycol at the OCP. The Bode and Nyquist plots for duplex steel sample in 100 ppm NaCl solution with different concentrations of ethylene glycol are shown in Fig. 3 and Fig. 4. Bode diagrams reveal that the impedance data consist of one time constant. A depressed capacitive loop in impedance diagrams is due to the charge transfer resistance and the double layer capacitance. The equivalent circuit compatible with the Nyquist diagram recorded in the presence of ethylene glycol is presented in Fig. 5. Constant phase element (CPE) Q_{dl}, R_s and R_{ct} can be corresponded to double layer capacitance, solution resistance, and charge transfer resistance, respectively. The simplest approach requires the theoretical transfer function $Z(\omega)$ which can be represented by a parallel combination of a resistance R_{ct} and a capacitance C, both in series with another resistance R_s:[19]

$$Z(w) = R_s + \frac{1}{R_{ct}^{-1} + iwC} \qquad (1)$$

To obtain a satisfactory impedance simulation of stainless steel alloy, it is necessary to replace the capacitor (C) with a constant phase element (CPE) Q in the equivalent circuit. The most widely accepted explanation for the presence of CPE behavior and depressed semicircles on solid electrodes is microscopic roughness, causing an inhomogeneous distribution in the solution resistance as well as in the double-layer capacitance.[20,21]

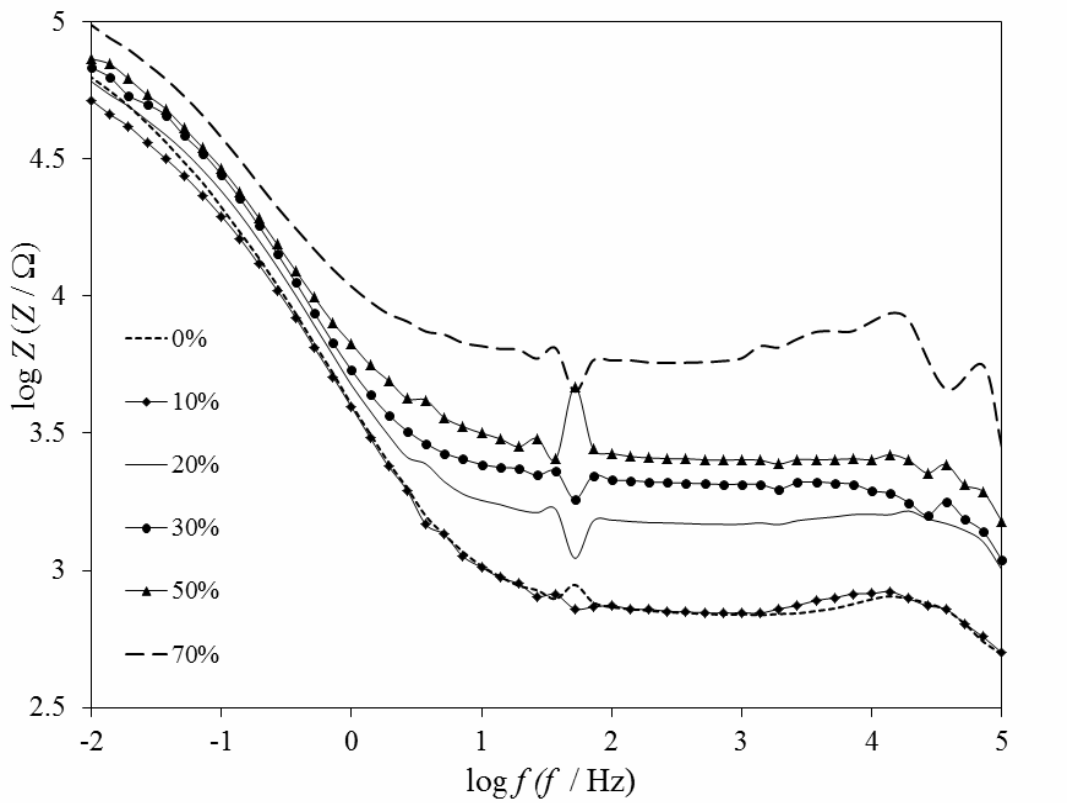

Fig. 3 – Bode diagrams of duplex steel alloy electrode in 100 ppm NaCl
and ethylene glycol-water solution at different concentrations of ethylene glycol.

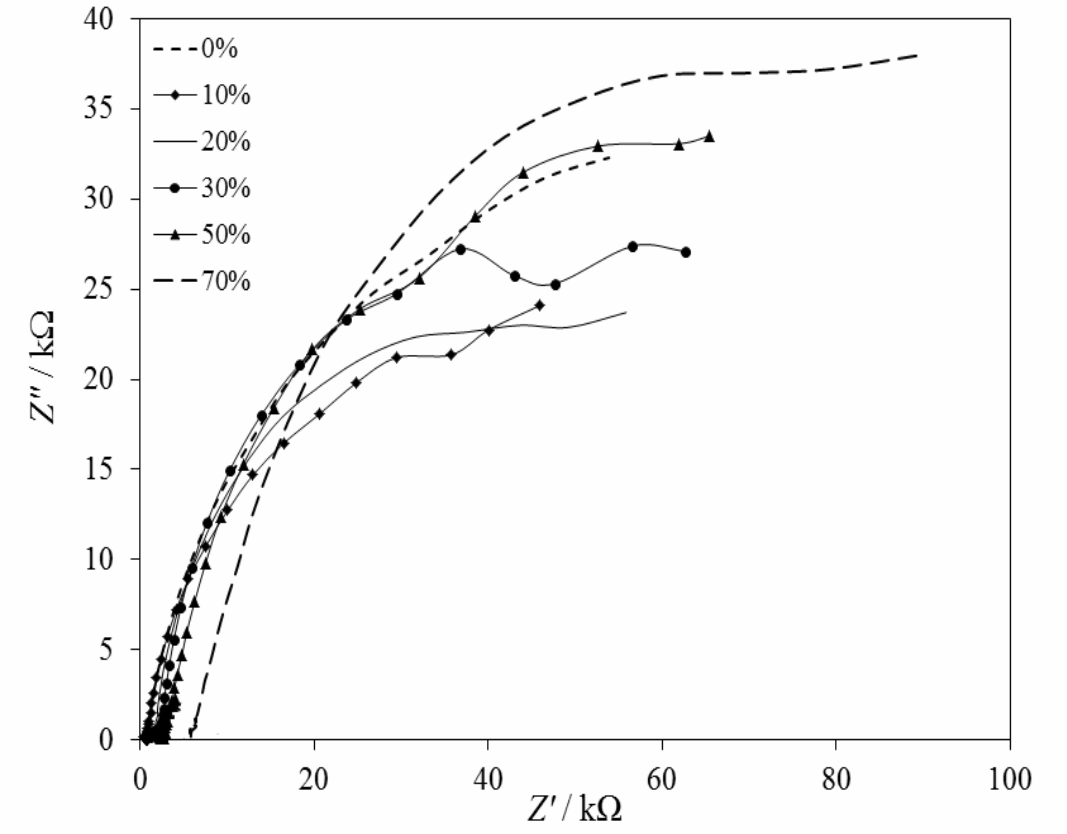

Fig. 4 – Nyquist diagrams of duplex steel alloy electrode in 100 ppm NaCl and ethylene glycol-water solution
with different concentrations of ethylene glycol.

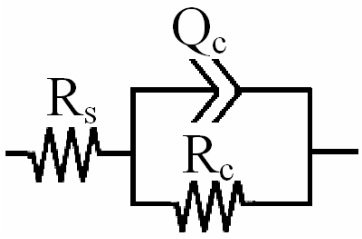

Fig. 5 – Equivalent circuits compatible with the experimental impedance data for corrosion of duplex steel alloy electrode in ethylene glycol solution.

Table 3

Equivalent circuit parameters in the corrosion of steel alloy in 100 ppm NaCl and ethylene glycol-water solution with different concentrations of ethylene glycol

Ethylene glycol % V/V	R_S /Ω	R_{ct} / 10^4 Ω	Q_{dl} / 10^{-5} F	n
0	712	7.9	6.2	0.79
10	727	5.8	6.4	0.80
20	1492	6.5	5.3	0.81
30	2005	7.6	4.8	0.81
50	2601	10.3	4.6	0.72
70	6661	10.8	3.6	0.78

The impedance plots obviously confirm the polarization results. It can be shown that the charge transfer resistance, R_{ct}, increases significantly with increasing ethylene glycol concentration. To authenticate the equivalent circuit, the experimental data are fitted to equivalent circuit and the circuit elements are obtained. Table 3 illustrates the equivalent circuit parameters for the impedance spectra of corrosion of steel alloy in ethylene glycol solution. From Table 3, with increasing the ethylene glycol concentration, the solution resistances (R_s) increase. Pure ethylene glycol has very poor electrical conductivity and is almost an insulator. Therefore, the resistivity of ethylene glycol solution increases with the increase in ethylene glycol content. In addition, the dilution by subjoining the water to solution facilitates the hydrolysis of the hydroxyl groups of ethylene glycol which lead to increasing electrical conductivity.

With increasing in ethylene glycol concentration to 10%, the charge transfer resistance decreases. Moreover, in higher concentration of ethylene glycol, the charge transfer resistance increases. Also, it can be seen that the polarization resistance of steel alloy in an ethylene glycol solution would be dependent on the solution resistance. As the solution resistance increases with an increase the concentration of ethylene glycol, the polarization resistance increases.[18]

Like most other organic compounds, ethylene glycol should be easily adsorbed on surface of electrode.[22] The double layer capacitance is a good indication of the adsorption of ethylene glycol on steel alloy surface. Q_{dl} can be easily calculated based on the equivalent circuit of the measured EIS. It appears that the capacitance tends to decrease as the ethylene glycol concentration increases. This indicates a change at the steel alloy/solution interface. A decreasing interface capacitance can be caused by high dielectric water at the interface being replaced by some substance that is larger in molecular size. Ethylene glycol molecule is larger than water, so the adsorption of the ethylene glycol molecules at the surface of steel alloy can result in a lower Q_{dl}. When the concentration of ethylene glycol increases, more ethylene glycol will be adsorbed on the surface of electrode, leading to a lower Q_{dl}. In other words, the steel alloy surface is more completely covered by ethylene glycol in a more concentrated ethylene glycol solution. This explains the decreasing corrosion rate of steel alloy with increasing concentration of ethylene glycol.

Current-potential characteristics resulting from cathodic and anodic polarization curves of duplex stainless steel in 10% ethylene glycol solution at various temperatures are shown in Fig. 6 and the corresponding polarization parameters are listed in Table 4. It is seen that corrosion potentials shift to more negative values with increasing the solution temperature. Furthermore, under the same cathodic and anodic polarization potential, the cathodic and anodic current densities increase remarkably in higher solution temperature. The increasing solution temperature would accelerate both the cathodic reduction and anodic oxidation reaction.[22]

The effect of temperature on the corrosion reaction is very complex, because many changes occur on the metal surface. The change of the corrosion current at selected concentrations of the ethylene glycol was studied in 100 ppm NaCl solution at different temperatures (293, 313,333 and 353 K) and the results were listed in Table 5. In the presence of the ethylene glycol, the corrosion current of steel alloy decreases at any given temperature as the ethylene glycol concentration increases due to the increase in the degree of surface coverage. In contrast, at constant ethylene glycol concentration, with increasing temperature, the corrosion current density increases.

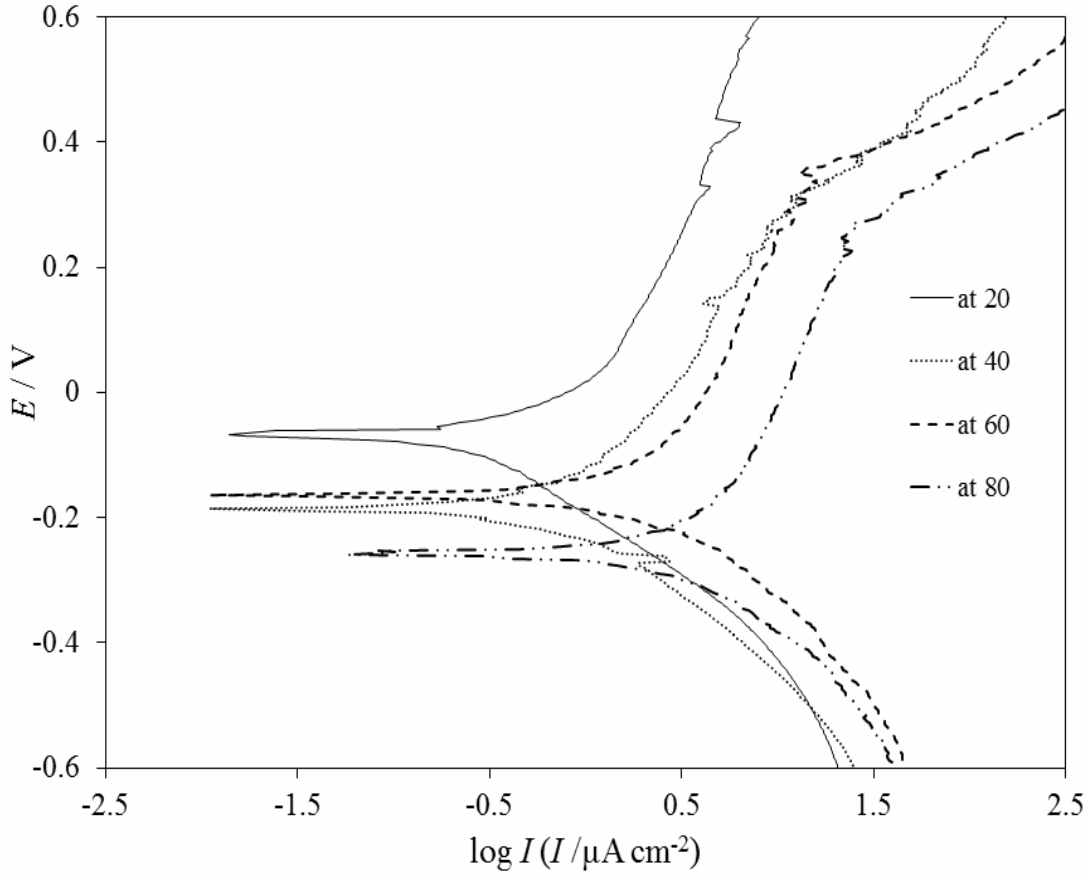

Fig. 6 – Polarization curves of duplex stainless steel electrode in 100 ppm NaCl and 10% ethylene glycol-water solution at different temperature.

Table 4

Polarization parameters in the corrosion of steel alloy in 100 ppm NaCl and ethylene glycol-water solution in 10% ethylene glycol solution at various temperatures

Temperature / ºC	E_{corr} / V	I_{corr} / μA cm^{-2}	R_p / kΩ	β_a / V dec^{-1}	β_c / V dec^{-1}	CR / mm year^{-1}
20	-0.075	0.55	40.1	0.185	0.07	0.006388
40	-0.187	0.75	29.6	0.19	0.08	0.0086964
60	-0.204	1.21	21.2	0.21	0.082	0.014065
80	-0.258	1.64	17.9	0.21	0.1	0.019005

Table 5

Corrosion current density of 2205duplex stainless steel alloy in 100 ppm NaCl with different ethylene glycol concentration and different temperature

Ethylene glycol % V/V	I_{corr} (293K) / μA cm^{-2}	I_{corr} (313 K) / μA cm^{-2}	I_{corr} (333 K) / μA cm^{-2}	I_{corr} (353 K) / μA cm^{-2}
10	0.55	0.75	1.21	1.64
30	0.197	0.283	0.559	0.675
50	0.139	0.195	0.48	0.575

To calculate activation thermodynamic parameters of the corrosion process, Arrhenius Eq. (2) and transition state Eq. (3) were used:[23-25]

$$I_{corr} = K_a \exp(\frac{E_a}{RT}) \quad (2)$$

$$I_{corr} = \frac{RT}{NH} \exp(\frac{\Delta S_a}{T}) \exp(\frac{-\Delta H_a}{RT}) \quad (3)$$

where E_a is the apparent activation energy of corrosion, R is the universal gas constant, K_a is the Arrhenius pre-exponential factor, H is the Plank's constant, N is the Avogadro's number, ΔS_a is the entropy of activation and ΔH_a is the enthalpy of activation.

Values of apparent activation energy of corrosion (E_a) for steel alloy in the absence and presence of various concentrations of ethylene glycol were determined from the slope of ln(I_{corr}) vs. T^{1} plots (Fig. 7) and shown in Table 6. The increase in activation energy with increasing ethylene glycol concentrations indicates that the physical adsorption (electrostatic) occurs in the first stage. Also the plots of ln(I_{corr} T^{-1}) against T^{-1} (Fig. 8) give a straight line with a slope of (-ΔH_a R^{-1}) and an intercept of (ln$R$ N^{-1} h^{-1}+ ΔS_a R^{-1}) from which the values of ΔH_a and ΔS_a are calculated and are listed in Table 6. One can notice that E_a and ΔH_a values vary in the same way. This result permits to verify the known thermodynamic relation between the E_a and ΔH_a as shown in Table 6:[24]

$$\Delta H_a = E_a - RT \quad (4)$$

On the other hand, ΔS_a decreases with increasing ethylene glycol concentrations (Table 6). The negative values of entropies imply that a decrease in disordering takes place on going from reactants to the adsorbed system.[24] The positive values of ΔH_a mean that the dissolution reaction is an endothermic process. In addition, an increase in ethylene glycol concentration leads to higher values of ΔH_a.

CONCLUSIONS

The corrosion behavior of duplex stainless steel alloy 2205 was studied through electrochemical methods in ethylene glycol-water mixture at different concentrations and temperatures. The results revealed that corrosion potentials shifted to positive values with increase the concentration of ethylene glycol. With increase in the concentration of ethylene glycol to 10%V/V, corrosion current of steel alloy substrate increased. In the higher ethylene glycol concentration, corrosion rate of duplex steel alloy decreased. Electrochemical impedance spectroscopy at different ethylene glycol concentrations showed that the double layer capacitance tended to decrease as the ethylene glycol concentration increased.

With increasing the temperature, corrosion current increased and the corrosion potentials shifted toward more negative values. Thermodynamic parameters indicated that the dissolution reaction was an endothermic process.

Table 6

Values of activation parameters E_a, ΔH_a and ΔS_a for 2205 steel alloy in 100 ppm NaCl at different concentration of ethylene glycol

Ethylene glycol % V/V	K_a / mA cm^{-2}	E_a / kJ mol^{-1}	ΔH_a / kJ mol^{-1}	ΔS_a / kJ mol^{-1}K^{-1}	$RT=E_a$ - ΔH_a / kJ mol^{-1}
10	0. 394	16.1	13.44	-0.319	2.66
30	0. 439	18.9	16.19	-0.318	2.71
50	0. 894	21.3	18.61	-0.313	2.69

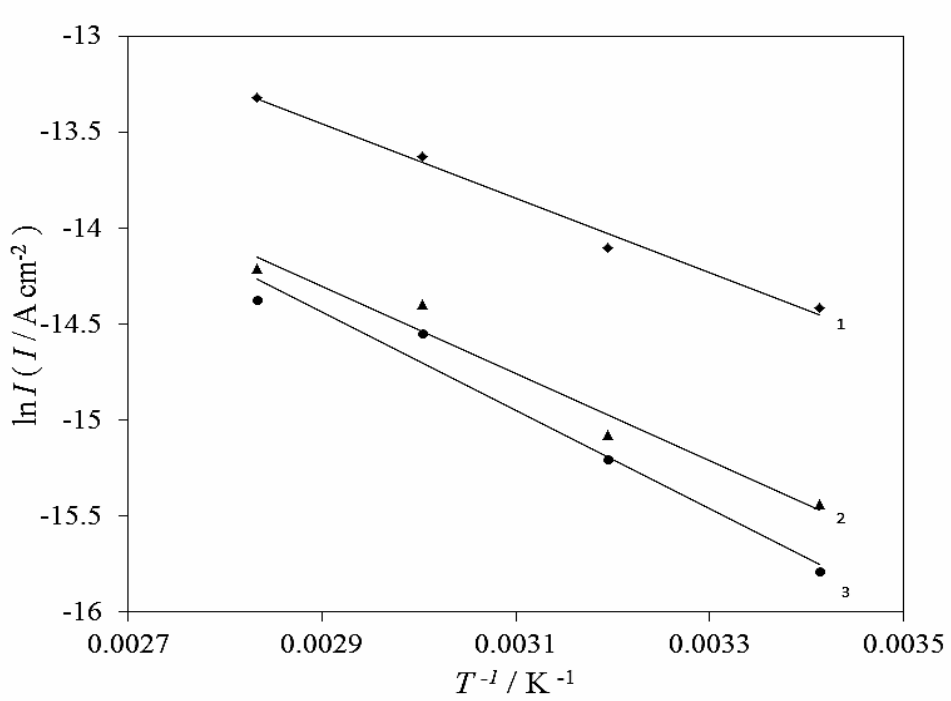

Fig. 7 – Typical Arrhenius plots of $\ln(I_{cort})$ vs. T^{-1} for steel alloy in 100×10^{-6} NaCl at different concentrations of ethylene glycol: 1: 10; 2: 30; 3: 50 %V/V ethylene glycol.

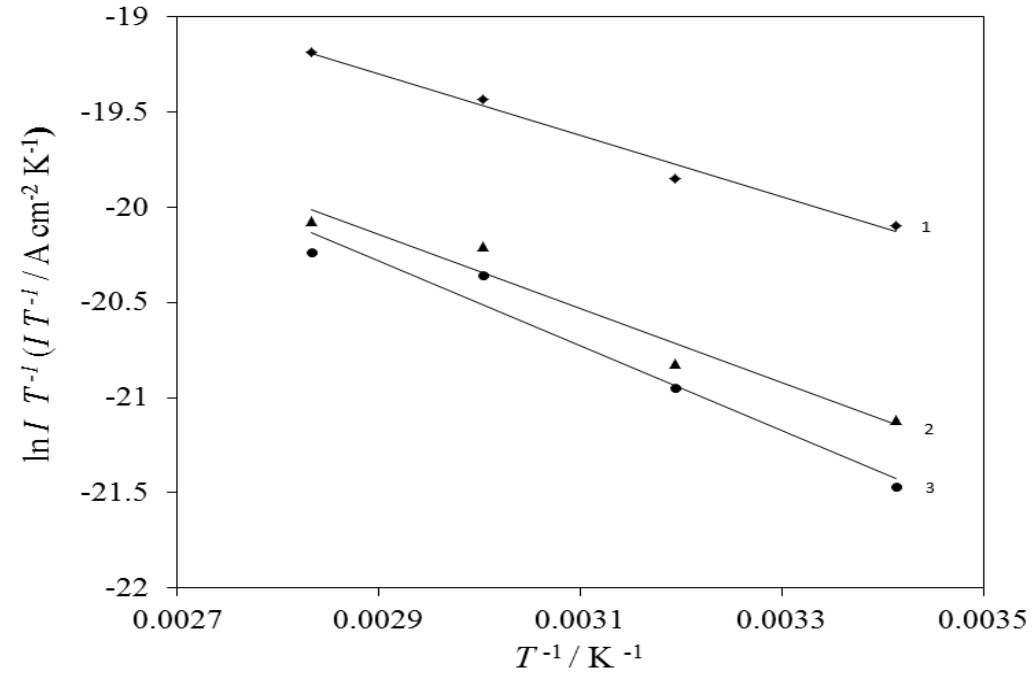

Fig. 8 – Typical Arrhenius plots of $\ln(I_{corr}T^{1})$ vs. T^{1} for steel alloy in 100 ppm NaCl at different concentrations of ethylene glycol: 1: 10; 2: 30; 3: 50 %V/V ethylene glycol.

REFERENCES

1. G. Bolat, A. Cailean, D. Sutiman and D. Mareci, *Rev. Roum. Chim.,* **2014**, *59*, 53.
2. F. Branzoi and V. Branzoi, *Rev. Roum. Chim.,* **2014**, *59*, 299.
3. L. Jinlong, L. Tongxiang, D. Limin and W. Chen, *Corros. Sci.*, **2016**, *104*, 144.
4. H. J. Kim, S. H. Jeon, S. T. Kim, I.S. Lee, Y.S. Park, K.T. Kim and Y.S. Kim, *Corros. Sci.*, **2014**, *87*, 60.
5. I. Danaee and M. Niknejad Khomami, *Material Wiss. Werkst.,* **2012**, *43*, 942.
6. L.Y. Xu and Y.F. Cheng, *Corros. Sci.*, **2008**, *50*, 2094.
7. S. Tierce, N. Pébere, C. Blanc, C. Casenave, G. Mankowski and H. Robidou, *Corros. Sci.,* **2007**, *49*, 4581.

8. I. Danaee, M. Niknejad Khomami and A. A. Attar, *J. Mater. Sci. Technol.*, **2013**, *29*, 89.
9. O.K. Abiola and J.O.E. Otaigbe, *Corros. Sci.*, **2008**, *50*, 242.
10. E. Samiento-Bustos, J.G. González Rodriguez, J. Uruchurtu, G. Dominguez-Patiño and V.M. Salinas-Bravo, *Corros. Sci.*, **2008**, *50*, 2296.
11. I. Danaee, M. Niknejad Khomami and A. A. Attar, *Mater. Chem. Phys.,* **2012**, *135*, 658.
12. S. Tierce, N. Pébere, C. Blanc, C. Casenave, G. Mankowski and H. Robidou, *Electrochim. Acta,* **2006**, *52*, 1092.
13. K. Ranjbar and A. Abasi, *Eng. Fail. Anal.,* **2013**, *31*, 161.
14. E. Guilminot, F. Dalard and C. Degrigny, *Corros. Sci.,* **2002**, *44*, 2199.
15. E. Samiento-Bustos, J.G. González-Rodriguez, J. Uruchurtu and V.M. Salinas-Bravo, *Corros. Sci.,* **2009**, *51*, 1107.
16. G. Song and D. StJohn, *Corros. Sci.,* **2004**, *46*, 1381.
17. A. M. Fekry and M. Z. Fatayerji, *Electrochim. Acta,* **2009**, *54*, 6522.
18. H. Jafari, I. Danae, H. Eskandari and M. RashvandAvei, *Ind. Eng. Chem. Res.,* **2013**, *52*, 6617.
19. M. Kazemi, I. Danaee and D. Zaarei, *Material Wiss. Werkst.,* **2014**, *45*, 574.
20. F. Branzoi and V. Branzoi, *Rev. Roum. Chim.*, **2015**, *60*, 85.
21. S. Iacoban, G. Bolat, C. Munteanu, D. Cailean, L. Trinca and D. Mareci, *Rev. Roum. Chim.,* **2015**, *60*, 949.
22. M. Gholami, I. Danaee, M. H. Maddahy and M. Rashvandavei, *Ind. Eng. Chem. Res.,* **2013**, *52*, 14875.
23. A.R. Hoseinzadeh, I. Danaee and M.H. Maddahy, *J. Mater. Sci. Technol.*, **2013**, *29*, 884.
24. H. Jafari, I. Danaee, H. Eskandari and M. Mehdi RashvandAvei, *J. Mater. Sci. Technol.*, **2014**, *30*, 239.
25. P. Kumarip, P. Shetty, S. Arao and D. Sunil, *Rev. Roum. Chim.,* **2014**, *59*, 323.